buildings

Article

Real-Time Monitoring of Concrete Vibration Depth Based on RFID Scales

Yuhu Quan [1], Xinzhi Wang [2], Yancheng Liu [2], Hongpeng Sun [2] and Fenglai Wang [1,3,4,*]

[1] School of Civil Engineering, Harbin Institute of Technology, Harbin 150090, China; quanyuhuhit@outlook.com
[2] Long Jian Road & Bridge Co., Ltd., Harbin 150090, China
[3] Key Lab of Structures Dynamic Behavior and Control of the Ministry of Education, Harbin Institute of Technology, Harbin 150090, China
[4] Key Lab Smart Prevention and Mitigation of Civil Engineering Disasters of the Ministry of Industry and Information Technology, Harbin Institute of Technology, Harbin 150090, China
* Correspondence: fl-wang@hit.edu.cn

Abstract: The vibration of concrete is a typical concealed construction process, in which mature supervisory methods are lacking. The quality of vibration relies heavily on the subjective experience and sense of responsibility of the vibration operators. For the widely used hand-held concrete vibrators, existing methods for monitoring the quality of vibration primarily focus on the horizontal positioning of the vibrator. Due to the limited measurable range of vibration depth, these methods are inapplicable for monitoring the vibration depth during the vibration of deeper structures such as walls, columns, and large volumes of concrete. This paper makes the initial attempt to address the issue of monitoring concrete vibration depth, presenting a method that broadens the measurable range of depth in vibration monitoring. Inspired by the principles of optical and magnetic scales, this paper introduces a radio frequency identification (RFID) scales positioning system for the real-time monitoring of vibration depth. The proposed RFID scales vibration depth monitoring method theoretically has no upper limit on the measurable vibration depth, rendering it applicable to monitoring vibration depth of any extent. By comparing the positioning accuracy of different RFID scales hardware compositions, the optimal RFID scales hardware composition and the most effective RFID scales positioning algorithm were identified. The feasibility and accuracy of the vibration depth monitoring method based on RFID scales were validated through engineering field application. This method achieves centimeter-level accuracy in monitoring vibration depth, offers a tool for the precise control of vibration depth, and helps avoid potential quality issues in vibration.

Keywords: concrete vibration; vibration depth monitoring; RFID scales; quality control

Citation: Quan, Y.; Wang, X.; Liu, Y.; Sun, H.; Wang, F. Real-Time Monitoring of Concrete Vibration Depth Based on RFID Scales. *Buildings* **2024**, *14*, 885. https://doi.org/10.3390/buildings14040885

Academic Editor: Shaohong Cheng

Received: 12 February 2024
Revised: 15 March 2024
Accepted: 20 March 2024
Published: 25 March 2024

1. Introduction

Concrete vibration is an essential step in civil engineering construction. It is a critical procedure for both precast and cast-in-place concrete structures. Once concrete is poured into the formwork, it must be vibrated to eliminate air bubbles and voids in the freshly poured concrete [1], ensuring the compactness and uniformity of the material [2,3]. The quality of vibration directly influences the quality and durability of the final structure.

Hand-held concrete vibrators are applicable to a wide range of engineering structures due to their versatility in accommodating various irregular and confined spaces, making them the most widely used equipment for concrete vibration. During vibration, the vibrator must be inserted to a specified depth within the concrete to achieve the desired compaction. Construction standards and codes from various countries [4–6] have detailed requirements for the position, depth, duration, and technique of vibrator use. However, vibration is a concealed construction process, and whether the vibrator reaches the predetermined depth inside the concrete cannot be directly observed by the naked eye. The quality of vibration lacks mature technical methods for monitoring and evaluation and is dependent on the vibration personnel's subjective judgment and sense of responsibility. This increases the potential risk of quality issues in the concrete vibration process.

With the advent of the smart construction era, the current frontier in concrete vibration construction research is to objectively evaluate the quality of vibration using digital methods and a variety of Internet of Things (IoT) sensors [7]. The monitoring data of concrete vibration are fundamental for further research, such as assessing the degree of compaction [8] and modeling the distribution of aggregates within the concrete [9]. The key indicators of vibration monitoring are the vibration location, duration, and technique [10]. The vibration location includes both the horizontal position and the vibration depth. The vibration technique demands that the concrete vibrator should be quickly inserted and slowly withdrawn—fast insertion before vibration and slow withdrawal afterward—to avoid creating new voids or holes in the freshly vibrated concrete. The vibration technique is primarily related to the depth of vibration and the time taken to insert and withdraw the vibrator.

Current research and solutions for vibration monitoring are predominantly focused on the horizontal positioning of the vibrator. Positioning sensors, such as satellite positioning antennas [11] and ultra-wideband (UWB) positioning modules [12,13], have been affixed to concrete vibrators to achieve accurate tracking of the vibrator's horizontal location and depth. As wireless signals from positioning sensors cannot propagate through steel-reinforced concrete, the sensors must be kept external to the concrete, thus constraining the maximum insertion depth of the vibrator. Consequently, these solutions are unsuitable for scenarios where the vibrator needs to be fully inserted into the concrete. Additionally, the physical bulk of these sensors hinders the vibrator's insertion into tight and irregular spaces within structures. Another approach involves predicting the position of a hand-held vibrator based on the operator's posture and shoulder positioning [14]. However, due to the flexibility of the vibrator's shaft, the operator's posture does not change once the vibrator is inserted beyond a certain depth, making this method suitable only for shallow-depth concrete vibration monitoring.

Actually, there is an urgent need for monitoring the vibration depth at deeper depths, yet there is a lack of research and solutions in this area. Zhang et al. [15] have investigated the impact of vibration depth on the lateral pressure against concrete formwork, introducing for the first time the concept of ultra-deep vibration: it occurs when the insertion depth of the vibrator exceeds the effective head height of the poured concrete. Ultra-deep vibration significantly increases the lateral pressure exerted on the formwork during vibration [16], necessitating strict control over the vibration depth. In the layered vibration of large-volume concrete, the vibrator must be inserted 5–10 cm into the preceding concrete layer to ensure good overlap between layers [6]. Since the interior of the concrete cannot be directly observed, it is challenging to accurately control vibration depth based solely on the experience of the vibration personnel. Therefore, achieving depth monitoring of concrete vibration at any depth is fundamental to ensuring the safety and quality of concrete vibration construction.

This study proposes an RFID scales positioning system based on ultra-high frequency radio-frequency identification (UHF-RFID) technology for monitoring the vibration depth in various deeper structures. UHF-RFID technology has the advantage of long recognition distances, a wide identification range, and signals with penetrability, allowing for the rapid identification of a large number of RFID tags in a short time. It is widely used in scenarios such as logistics [17], inventory management [18], construction management [19], object tracking [20,21], and indoor positioning [22,23]. Inspired by optical and magnetic scales, the RFID scales positioning system creates an RFID scales strip by arranging a series of RFID tags. By recognizing RFID tag signals within a certain range through an RFID antenna, the system achieves the positioning of the antenna by exploiting the signal strength differences between the detected tags.

Optical scales [24] and magnetic scales [25] consist of continuous gratings and magnetic strips, respectively. Positioning of the read head is achieved by identifying the changing grating patterns and magnetic field signals through the read head. Optical scales require an unobstructed line of sight between the strip and the read head, while magnetic scales necessitate precise alignment between the read head and the strip to ensure the continuous detection of magnetic signals. However, the imperfect conditions at concrete vibration construction sites, which can contaminate the scales strips, make it impractical to apply optical or magnetic scales for measuring concrete vibration depth. Due to the penetrative nature of UHF-RFID signals, the RFID scales can still operate stably when there is some cementitious mortar between the RFID scales strip and the reader. Therefore, the vibration depth monitoring method based on RFID scales can achieve depth monitoring of concrete vibration at any depth. Additionally, the RFID scales strip uses thin-film RFID tags. The vibrator equipped with the RFID scales strip can still be inserted into narrow structures for concrete vibration.

The subsequent sections of this paper are organized as follows. Section 2 describes the hardware compositions of the RFID scales, the positioning algorithm, and the method of installing the RFID scales on the hand-held concrete vibrator. Section 3 validates the centimeter-level positioning accuracy of the RFID scales by laboratory experiments and verifies the feasibility of using the RFID scales for vibration depth monitoring in field applications. Section 4 discusses the innovations and future outlook of this paper. The last section provides the overall conclusions.

2. Materials and Methods

2.1. The Hardware Composition of RFID Scales

The optical scales consist of a series of etched gratings, and the position is determined by a photodetector read head that detects variations in the grating patterns and converts these changes into electrical signals. Magnetic scales are made up of uniformly spaced minute magnetic strips, and the read head can detect the changing magnetic poles between these magnetic strips, thereby determining the read head's position. Their positioning principle is to measure displacement by detecting the location of the read head on the strip. Inspired by this, a series of flexible RFID tags are arranged at fixed intervals to form a strip. Each RFID tag is encoded with a unique identification number. An RFID antenna coupled with an RFID reader constitutes the read head. By detecting the identification numbers of the RFID tags around the antenna, the position of the read head on the RFID tag strip can be determined. This RFID-based positioning system is named the RFID scales, as shown in Figure 1.

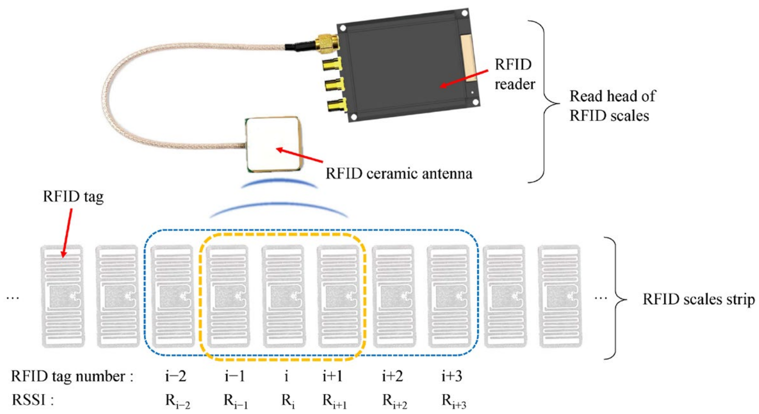

Figure 1. The composition of RFID scales. The blue frame contains all the identified RFID tags. The orange frame contains the RFID tags selected by the algorithm for position calculation.

Optical scales and magnetic scales feature very fine scale intervals, achieving positioning accuracy of less than one millimeter. As a result, when optical and magnetic scales are in operation, the read head must be in close proximity to the scale strip to detect the signal, with the maximum installation gap for magnetic scale read heads being around 1 mm. In comparison, RFID scales has the following characteristics.

1. The RFID scales read head is composed of an UHF-RFID reader and an antenna, with adjustable power on the UHF-RFID reader, allowing it to read RFID tag signals within a range of several meters. This also means that a relatively large gap can exist between the RFID scales strip and the read head, and it can still function normally;
2. The space between the optical and magnetic scales read heads and the strips must be kept clean and uncontaminated to function properly. In contrast, the wireless signal from the RFID scales read head antenna can penetrate the cement mortar layer covering the RFID scales strip, making it suitable for the vibration construction sites;
3. The width of RFID tags that make up the RFID scales strip are approximately 10 mm, which means the RFID scales can achieve centimeter-level positioning accuracy. Although the positioning accuracy of the RFID scales is lower compared to that of optical and magnetic scales, the RFID scales has a farther recognition distance and can function stably in worse construction environment. The RFID scales strikes a balance between positioning accuracy and working conditions. For concrete vibration, centimeter-level depth monitoring accuracy is already sufficient.

2.2. Digital Board—External Vibration Depth Monitoring Equipment

To apply the RFID scales to the monitoring of vibration depth, this paper proposes a sensor installation method called the digital board. The RFID scales read head is installed on a slender, external board. The design of the digital board is simple and user-friendly, achieving the monitoring of vibration depth without the need for any additional equipment.

As in Figure 2, the digital board is a rectangular board with a central opening. When the vibrator is inserted into the concrete, the digital board is placed on the top of the formwork or rebar at the insertion point. The vibrator passes through the central opening of the digital board and is inserted into the concrete for the vibration process. The digital board remains stationary while the vibrator is inserted, in operation, and withdrawn from the concrete. Once the vibrator is completely withdrawn from the concrete, during the moving to the next insertion point, the digital board hangs at the junction of the vibrator's metal head and the flexible shaft, following the vibrator to the next vibration location. Because the diameter of the digital board's opening is smaller than that of the metal head but larger than the diameter of the flexible shaft, the digital board will not slip off the metal head and can move freely along the flexible shaft.

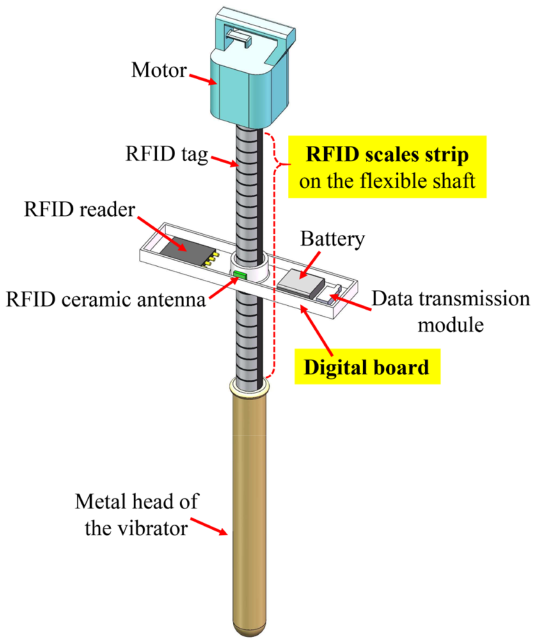

Figure 2. Digital board—external vibration depth monitoring equipment.

The RFID scales strip is composed of a series of flexible, waterproof RFID tags, which are wrapped and affixed at equal intervals d along the flexible shaft of the concrete vibrator, as shown in Figure 2. The first RFID tag, located at the junction between the flexible shaft and the vibrator head, is numbered 0, and the distance from this tag to the top end of the vibrator head is S. Along the direction of the flexible shaft, the corresponding numbers of the tags increase sequentially. The distance from the tag numbered i to the top end of the vibrator metal head is given by the expression $D_i = i \cdot d + S$. Each tag has a unique identification number, which can be used to determine the distance from the tag to the top end of the vibrator head.

As shown in Figure 2, the RFID antenna of the RFID scales read head is mounted on the sidewall of the digital board's opening, directly facing the RFID scales strip. By real-time reading of the RFID tag number at the digital board's opening, the real-time distance from the top end of the vibrator head to the digital board can be determined. This distance is the real-time vibration depth of the concrete vibrator from the top of the structure into the concrete.

During vibration construction, the digital board may rotate around the flexible shaft. To ensure optimal RFID tag recognition, it is necessary to maintain the RFID antenna facing at least a portion of the RFID tag at all times. Therefore, when affixing the RFID tags around the flexible shaft, the tag should cover as much of the shaft's circumference as possible. Actually, manufacturers can produce RFID tags of various lengths according to requirements. On the flexible shaft of the vibrator, the RFID scales strip at the same location can use one long RFID tag or 2–3 short RFID tags arranged consecutively to wrap around the shaft, achieving the same coverage effect.

In fact, due to the RFID tags being flexibly wrapped and arranged around the vibrator's flexible shaft, there is a difference in the recognition sensitivity between long and short RFID tags. This sensitivity also varies according to the type and size of the RFID antenna. To achieve the best RFID recognition performance and the highest RFID scales positioning accuracy during concrete vibration, three types of RFID antennas and three RFID scales strip composition schemes were tested in Section 3.1. The optimal RFID scales composition for monitoring vibration depth was found. Using a single ceramic antenna and a dual-tag RFID scales strip composition scheme, depth measurement accuracy of 3.6 cm can be achieved stably.

Moreover, the digital board integrates power supply and data transmission modules, enabling real-time wireless transmission of monitoring data to the remote terminal. The remote terminal can visualize the monitoring data in real-time for quality control. Meanwhile, the terminal will record and save the monitoring data on the hard drive, thereby creating the dataset of the vibration construction. In practical applications, the digital board has a waterproof cover that protects the electronic devices within, making it suitable for use in the harsh environment of concrete pouring and vibration. In the future, the digital board can also be equipped with a satellite positioning module or an ultra-wideband (UWB) positioning module. By locating and orienting the digital board, the spatial three-dimensional coordinates of the central opening of the digital board can be calculated in real time, achieving the monitoring of the horizontal position of the vibration insertion point. The location of the digital board goes beyond the scope of the research on vibration depth monitoring and will be addressed in future work.

2.3. Vibration Depth Measurement Algorithm of RFID Scales

According to the initial design, the vibration depth can be measured by real-time reading of the RFID tag number at the opening of the digital board. Actually, UHF-RFID is a technology for determining vicinity. Multiple RFID tags near the antenna can be identified simultaneously in one detection. In other words, RFID technology can only determine the approximate location near which RFID tags through the identification and cannot directly provide an accurate location.

In previous studies, the fundamental principle of the RFID positioning system is to convert the received signal strength indicator (RSSI) values or phase information of the detected tags into the distance between the antenna and the tags [26]. Then, the coordinates of the antenna or tag can be calculated using numerical algorithms such as trilateration.

In this study, the vibration depth measurement algorithm of RFID scales is proposed. Using the RSSI values of the detected tags, each tag's weight is calculated through an exponential weighting method. By taking a weighted average of the distance values represented by the tags, the corresponding numerical value on the RFID scales for the antenna can be determined. This weighted distance value is the current vibration depth.

As shown in Figure 3, the flowchart of the RFID scales depth algorithm sorts all detected tags in descending order based on RSSI values, selects the top k tags with the strongest RSSI signal strength, and calculates the weight of each tag by exponential weighting as in Equation (1).

$$w_i = \frac{e^{R_i}}{\sum\limits_{i \in A} e^{R_i}} \tag{1}$$

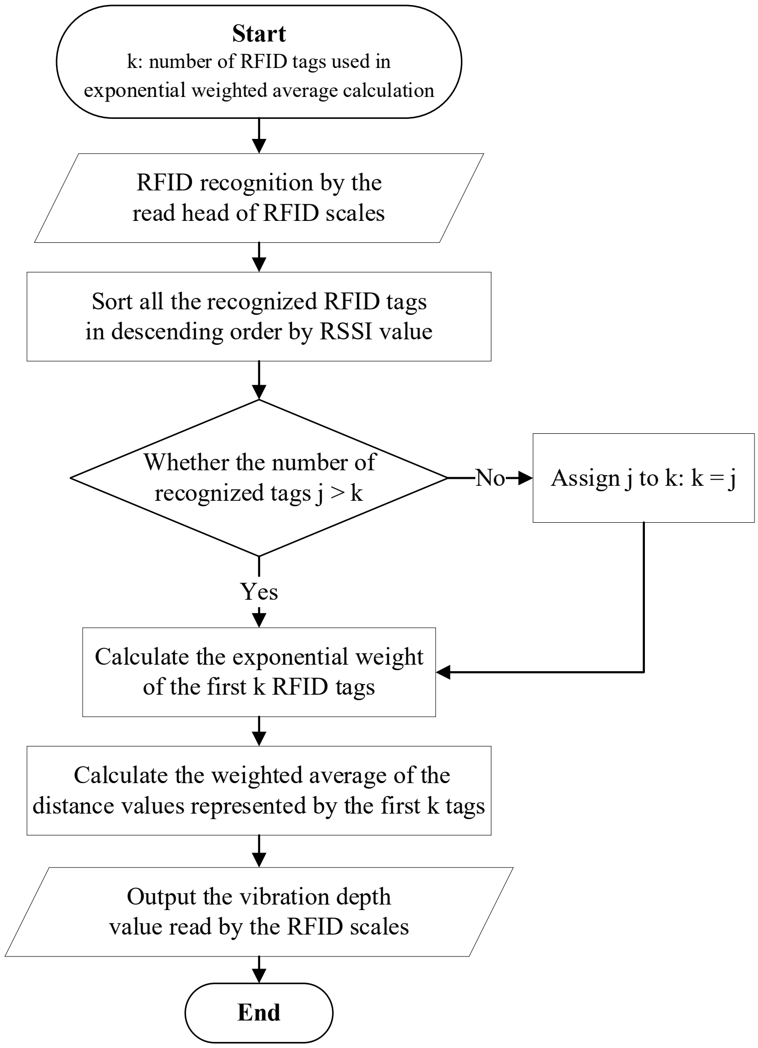

Figure 3. The flowchart of the RFID scales depth algorithm.

The set A = {number of the first k RFID tags sorted by RSSI}. R_i represents the RSSI value of the tag numbered i during detection.

The vibration depth value represented by the tag numbered i is expressed by Equation (2).

$$D_i = i \cdot d + S \tag{2}$$

The current vibration depth measured by the RFID scales can be calculated by Equation (3).

$$D_{depth} = \sum_{i \in A} w_i \cdot D_i = \frac{\sum\limits_{i \in A} e^{R_i} \cdot (i \cdot d + S)}{\sum\limits_{i \in A} e^{R_i}} \quad (3)$$

The depth algorithm of the RFID scales employs an exponential weighted average, where the exponent is used to amplify the weight differences between tags with varying RSSI values. The tag with the highest RSSI value is assigned the greatest proportion of weight, keeping the RFID scales positioning result near that tag. At the same time, this algorithm balances out the measurement errors in RSSI and avoids location errors that may arise from adjacent tags having similar RSSI values. In Section 3.2, the exponential weighting depth algorithm is further compared and analyzed against other positioning algorithms to illustrate its advantages and accuracy.

3. Experiments and Results

3.1. Experiment of Different RFID Scales Compositions

For the RFID scales strip, a series of RFID tags were wrapped and affixed at equal intervals along the flexible shaft of the vibrator. As mentioned above, at a specific location on the RFID scales, one long RFID tag or 2–3 short RFID tags can be used to wrap around the shaft. The antenna of the RFID scales read head can be a printed circuit board (PCB) antenna or a flat ceramic antenna of various sizes. The recognition performance and positioning accuracy of RFID scales are related to the RFID scales strip composition and the type of the antenna. In this section, a series of experiments were conducted to find the optimal hardware composition of the RFID scales.

When selecting antennas and strip tags, factors such as antenna recognition performance, recognition range, antenna volume, tag coverage area, impedance matching degree, and anti-interference performance were comprehensively considered. Finally, three typical types of RFID antennas and three RFID scales strips composed of different tags were selected for testing. In other words, a total of nine RFID scales hardware compositions were tested. The specifications of these antennas and tags are shown in Tables 1 and 2. Three RFID scales strips include a single-tag strip, a dual-tag strip, and a triple-tag strip. The single-tag strip consists of a single long RFID tag U9812 wrapped around the flexible shaft. For the dual-tag strip, two short RFID tags U4619 are wrapped around the flexible shaft at the same position. In the triple-tag strip, three short RFID tags U3314 are wrapped around the shaft at the same position. The three types of RFID antennas were the KLTXP7505 PCB antenna, the KLTX2018 ceramic antenna, and the slightly larger KLTX2525 ceramic antenna.

Table 1. The specification of three different RFID tags.

RFID Tag Type	Size	Reading Distance	Tag Chip	Tag Image
U9812 (Single-tag strip)	98 mm × 12 mm	0~6 m	NXP U8	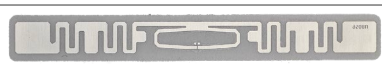
U4619 (Dual-tag strip)	46 mm × 19 mm	0~5 m	NXP U8	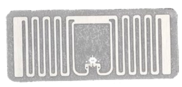
U3314 (Triple-tag strip)	33 mm × 14 mm	0~3 m	NXP U8	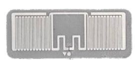

Table 2. The specification of three different RFID antennas.

Antenna Type	Material	Size	Power	Antenna Image
KLTXP7505	PCB	75 mm × 5 mm	1 dbi	
KLTX2018	ceramic	20 mm × 20 mm	1 dbi	
KLTX2525	ceramic	25 mm × 25 mm	1.5 dbi	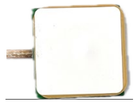

In addition, an RFID scales positioning accuracy test device was made, as shown in Figure 4. The device consists of a slide rail and a slider, with the RFID reader and antenna mounted on the slider. RFID tags are arranged on the flexible shaft of the vibrator to form RFID scales strip, with a 2.4 cm interval between the centers of each tag. The RFID scales strip is placed directly beneath the slide rail, allowing the antenna to move linearly along the rail to any position on the RFID scales. The height of the slide rail's ends can be adjusted to make sure that the distance between the RFID antenna and the strip is consistent with the actual distance during vibration.

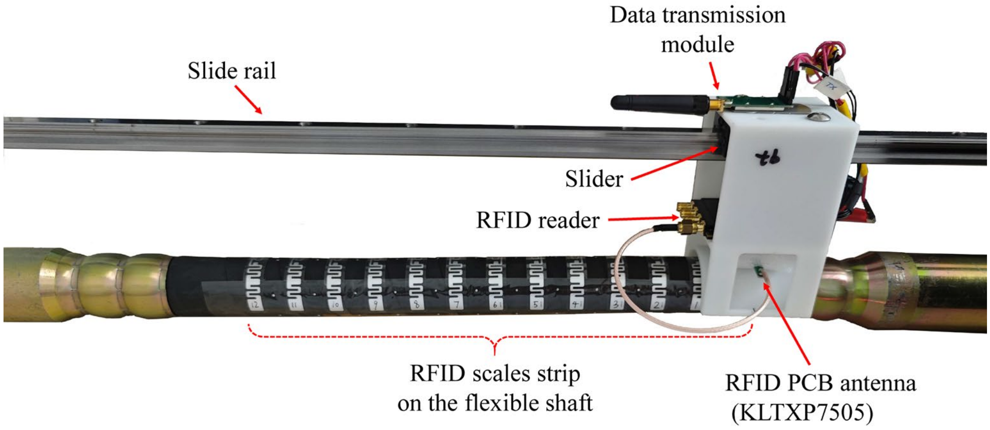

Figure 4. RFID scales positioning accuracy test device.

Although the width of the RFID tags used in the three RFID scales strips were not exactly the same, all the tags on the three types of strips were arranged at intervals of 2.4 cm, as shown in Figure 5. The RFID tag zone was defined as a range of 1.2 cm to the left and right of the tag's centerline, with a total width of 2.4 cm. Because of relative rotation between the concrete vibrator and the digital board, it is necessary to test the recognition performance of the RFID scales when the antenna faces different parts of the RFID scales strip, specifically when the antenna faces the center, the side, and the back of the tag.

The specific experimental steps are as follows:

1. Starting from the initial tag numbered 0, move the antenna along the slide rail so that the RFID antenna centerline can fall within different RFID tag zones. As the example in Figure 5, when the antenna centerline is moved to the zone of tag numbered i, activate the measurement function of the RFID read head, and record the identified tag numbers and RSSI values at that time. The recorded raw data are the input for the RFID scales depth measurement algorithm. Moreover, the tag number of the RFID tag zone where the antenna centerline is located is recorded as the target tag number. The recorded target tag number is similar to the ground truth in machine learning classification tasks, used for evaluating the accuracy of the RFID scales.
2. To ensure randomness of data collection, 4–5 measurements will be conducted within each RFID tag zone. For each measurement, the RFID antenna is moved along the slide

rail so that its centerline falls at any random position within the tag zone, and then, the RFID scales read head recognizes the nearby tags and records the measurement raw data.

3. When a round of measurements has been completed along the RFID scales strip from one end to the other, rotate the flexible shaft of the vibrator to adjust the part of the tag that the RFID antenna faces. Repeat the experiment step 2. Conduct the same measurements when the antenna faces the center, the side, and the back of the tag.
4. Test another RFID scales hardware composition, repeating steps 1, 2, and 3.

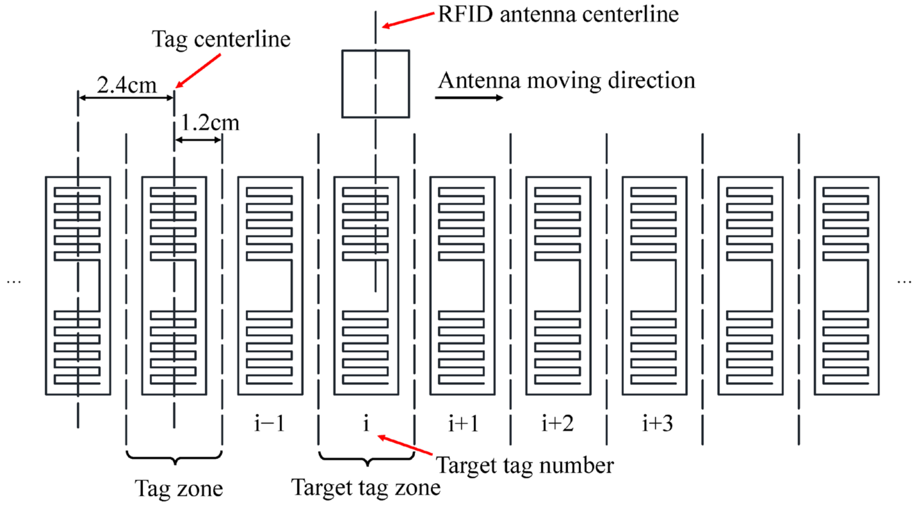

Figure 5. Schematic diagram of different RFID scales compositions experiment.

For concrete vibration depth monitoring, a measurement accuracy of centimeter level is sufficient. Therefore, no matter where the RFID antenna centerline is within the RFID tag zone, the RFID scales is expected to locate the current RFID tag zone which the RFID antenna centerline is in, which is also the RFID tag closest to the RFID antenna theoretically. Specifically, when the RFID antenna centerline is inside an RFID tag zone, the maximum deviation of the RFID antenna's real position from this tag center is 1.2 cm. If the RFID scales can locate the tag zone the antenna is in, it can be considered that the positioning accuracy of the RFID scales already meets the accuracy requirements for vibration depth monitoring.

3.2. RFID Scales Measurement Accuracy

In the RFID scales accuracy experiments, nine different RFID scales compositions were tested. The number of measurements conducted at various positions of the RFID scales for each composition is shown in Table 3. The experiment found that when the RFID scales adopted a single-tag strip scheme, neither type of ceramic antenna was able to detect the signal of the tag from the RFID scales strip when the shaft of the vibrator was rotated and the antenna faced the back of the tag. Therefore, there are seven effective RFID scales compositions available for comparative analysis.

Table 3. The number of measurements conducted for nine different RFID scales compositions.

RFID Scales Strip	RFID Antenna		
	PCB KLTXP7505	Ceramic KLTX2018	Ceramic KLTX2525
Single-tag strip	451	Unreadable for the back	Unreadable for the back
Dual-tag strip	340	325	326
Triple-tag strip	309	323	323

To compare the performance of different RFID scales and various positioning algorithms, two metrics are defined: accuracy rate (AR) and generalized accuracy rate (GAR). The accuracy rate refers to the ratio of the positioning result of RFID scales belonging to tag zone i when measurements are made in tag zone i. For the accuracy rate, the maximum deviation between the RFID scales positioning result and the actual location is 1.2 cm. The generalized accuracy rate refers to the ratio of the positioning result of RFID scales belonging to tag zone $i-1$, i, or $i+1$ when measurements are made in tag zone i. For the generalized accuracy rate, the maximum deviation between the RFID scales positioning result and the true position is 3.6 cm. In fact, the depth monitoring error within 3.6 cm is already sufficient for concrete vibration quality control.

As mentioned in Section 2.3, an exponential weighting positioning algorithm is used to process the detected RFID tag data. In order to further illustrate the advantage and necessity of the exponential weighting positioning algorithm, three different positioning algorithms were compared. The illustration of the three different positioning algorithms is presented in Table 4. Because the key of the RFID scales positioning system is how to handle the weight of different tags, the three chosen algorithms in Table 4 represent three typical methods of handling weights. For the maximum value algorithm, the weight of the RFID tag with the highest RSSI is 1, and the weight of other tags is 0. For the harmonic mean weighting algorithm, the weight difference between RFID tags is not significant, within an order of magnitude. For the exponential weighting algorithm, the weight of the RFID tag with the highest RSSI value is not within the same order of magnitude as the weights of other tags. The tag with the highest RSSI value is assigned the greatest proportion of weight. The accuracy of the maximum value algorithm, the harmonic mean weighting algorithm, and the exponential weighting algorithm is analyzed in detail in Section 3.3 through the error cumulative distribution function (CDF) diagram. Additionally, the optimal number of weights for the exponential weighting algorithm is determined.

Table 4. The illustration of the three different positioning algorithms for RFID scales.

Positioning Algorithm	Rules	Calculation Formula
Maximum value algorithm	The position of the RFID tag with the highest RSSI among the detected tags is taken as the positioning result for the RFID scales. When multiple tags have the same RSSI, the tag with the largest tag number is selected.	$\max_{i \in A}(R_i)$
Harmonic mean weighting algorithm	The top k RFID tags with the highest RSSI are taken, the harmonic mean weight of each tag is calculated. Perform the weighted average of the positions of these tags as the RFID scales positioning result.	$w_i = \frac{\frac{1}{R_i}}{\sum_{i \in A} \frac{1}{R_i}}$
Exponential weighting algorithm	The top k RFID tags with the highest RSSI are taken, the exponential weight of each tag is calculated. Perform the weighted average of the positions of these tags as the RFID scales positioning result.	$w_i = \frac{e^{R_i}}{\sum_{i \in A} e^{R_i}}$

The AR and GAR of three different positioning algorithms across various RFID scales hardware compositions are shown in Tables 5–7. For the harmonic mean weighting algorithm and the exponential weighting algorithm, Tables 6 and 7 also record the accuracy of using one to six different quantities of RFID tags for the weighted calculations to determine the optimal number of weights for these algorithms. In each table, the highest AR and GAR for each algorithm are highlighted in bold. According to Tables 5–7, the performance of RFID scales using PCB antenna KLTXP7505 and a single-tag strip is worse than other compositions in both AR and GAR. When the RFID scales consists of a ceramic antenna KLTX2018 and a triple-tag strip, the AR of all three algorithms reach their maximum, with little difference, all between 82% and 83%. For the GAR, when the RFID scales consists of a ceramic antenna KLTX2525 and a dual-tag strip, the GAR of all three algorithms reach the maximum, all above 99%. The geometric dimension of the ceramic antenna KLTX2018 is smaller than that of the ceramic antenna KLTX2525, and the size of the RFID tag U3314 used in the triple-tag strip is also smaller than the RFID tag U4619 used in the dual-tag strip. For the simplicity of description, the RFID scales composed of the ceramic antenna KLTX2018 and a triple-tag strip is called the small antenna small tag (SAST) scheme, and the RFID scales composed of the ceramic antenna KLTX2525 and a dual-tag strip is called the large antenna large tag (LALT) scheme. Thus, the best RFID scales composition should be chosen from either the SAST scheme or the LALT scheme.

Table 5. The accuracy rate (AR) and generalized accuracy rate (GAR) of maximum value algorithm.

RFID Scales Strip	RFID Antenna					
	PCB KLTXP7505		Ceramic KLTX2018		Ceramic KLTX2525	
	AR	GAR	AR	GAR	AR	GAR
Single-tag strip	47.45%	80.48%	Unreadable for the back		Unreadable for the back	
Dual-tag strip	45.59%	79.12%	60.31%	95.07%	58.59%	**99.38%**
Triple-tag strip	44.01%	71.84%	**82.66%**	92.88%	78.95%	96.59%

The bold numbers in the table indicate the maximum values of AR and GAR.

Table 6. The accuracy rate (AR) and generalized accuracy rate (GAR) of harmonic mean weighting algorithm.

RFID Scales Strip	Weighting Number	RFID Antenna					
		PCB KLTXP7505		Ceramic KLTX2018		Ceramic KLTX2525	
		AR	GAR	AR	GAR	AR	GAR
Single-tag strip	1	48.78%	81.37%	Unreadable for the back		Unreadable for the back	
	2	34.81%	80.04%				
	3	28.38%	76.27%				
	4	26.39%	70.51%				
	5	18.63%	63.41%				
	6	19.73%	52.77%				
Dual-tag strip	1	49.12%	83.53%	60.00%	97.23%	57.67%	**99.69%**
	2	42.35%	90.00%	70.15%	95.69%	71.17%	**99.39%**
	3	42.06%	87.94%	66.46%	95.69%	71.78%	98.77%
	4	31.47%	92.35%	68.62%	94.77%	72.70%	99.08%
	5	23.82%	88.82%	43.08%	93.54%	59.82%	97.55%
	6	24.41%	86.18%	42.46%	94.46%	58.90%	97.85%
Triple-tag strip	1	46.28%	78.32%	**82.04%**	92.57%	80.19%	95.98%
	2	43.69%	77.35%	79.57%	96.90%	79.88%	96.90%
	3	27.51%	82.20%	59.75%	94.74%	65.33%	94.12%
	4	23.30%	84.79%	61.61%	94.12%	72.14%	95.36%
	5	14.89%	78.32%	47.37%	94.12%	66.56%	94.43%
	6	11.00%	80.91%	43.96%	92.88%	58.82%	94.43%

The bold numbers in the table indicate the maximum values of AR and GAR.

For the SAST scheme, the smaller antenna size and the more densely arranged RFID tags allow the RFID read head to more sensitively detect the signal strength differences in RFID tags at different positions. This enables more refined RFID positioning measurements, leading to a higher AR of positioning. However, in terms of GAR, the LALT scheme is about 6% higher than the SAST scheme. This is because the larger RFID antenna and larger RFID tags can enhance the signal strength and stability of the detection for the target tag and its adjacent tags. The LALT scheme can more stably resist the impact of external interference on tag identification results. Therefore, as in Tables 6 and 7, the LALT scheme can significantly improve the GAR to 99.69% while slightly reducing the AR. This high GAR indicates that the positioning error of the RFID scales is almost controllable, with nearly 100% certainty that the positioning error of the LALT scheme is within the range of

3.6 cm. This ensures that the RFID scales positioning measurement result is smoother and more continuous, without abrupt data anomalies and jumps.

Table 7. The accuracy rate (AR) and generalized accuracy rate (GAR) of exponential weighting algorithm.

RFID Scales Strip	Weighting Number	RFID Antenna					
		PCB KLTXP7505		Ceramic KLTX2018		Ceramic KLTX2525	
		AR	GAR	AR	GAR	AR	GAR
Single-tag strip	1	48.78%	81.37%	Unreadable for the back		Unreadable for the back	
	2	44.78%	82.48%				
	3	45.90%	83.15%				
	4	46.34%	83.37%				
	5	46.56%	83.15%				
	6	46.56%	83.15%				
Dual-tag strip	1	49.12%	83.53%	60.00%	97.23%	57.67%	**99.69%**
	2	43.53%	88.53%	65.85%	96.62%	64.72%	99.39%
	3	42.65%	90.29%	66.46%	97.54%	65.34%	**99.69%**
	4	42.35%	90.59%	66.77%	97.23%	65.64%	**99.69%**
	5	42.65%	90.29%	66.77%	97.23%	65.64%	**99.69%**
	6	42.65%	90.59%	66.77%	97.23%	65.64%	**99.69%**
Triple-tag strip	1	46.28%	78.32%	82.04%	92.57%	80.19%	95.98%
	2	43.69%	77.35%	**82.97%**	95.05%	79.26%	96.28%
	3	44.66%	81.55%	82.66%	94.43%	80.19%	96.28%
	4	42.72%	82.52%	82.66%	94.74%	80.80%	96.28%
	5	42.07%	82.85%	**82.97%**	94.74%	80.19%	96.28%
	6	41.75%	83.17%	**82.97%**	94.74%	79.88%	96.28%

The bold numbers in the table indicate the maximum values of AR and GAR.

Based on the above reasons, as well as considering the harsh on-site construction environment during vibration, the LALT scheme is chosen as the best RFID scales hardware composition. This chosen RFID scales is composed of the ceramic antenna KLTX2525 and a dual-tag strip. The strong and stable RFID tag detection signal and controllable error of the LALT scheme make it the best choice for the RFID scales hardware composition.

3.3. Comparison with Other Positioning Algorithms

To further analyze the accuracy performance between various positioning algorithms, Figure 6 presents the error CDF diagram for three different positioning algorithms when using the LALT scheme. Since the maximum value algorithm can only position the antenna to a specific tag on the strip, the error CDF diagram for the maximum value algorithm can only be plotted in the form of star scatter points. As can be seen from the error CDF diagram, the GAR of the three positioning algorithms is almost the same. Both weighting algorithms have higher AR than the max algorithm. By assigning weights to multiple detected RFID tags, the weighting algorithms can eliminate random interference and noise encountered during RFID measurement to enhance positioning accuracy. Although the AR of the harmonic mean weighting algorithm is slightly higher by 5% compared to the exponential weighting algorithm, within the beginning of the error range, especially the error range of 0–1 cm, the error CDF for the exponential weighting algorithm is significantly higher than that of the harmonic mean weighting algorithm. This indicates that the positioning error of the exponential weighting algorithm is more concentrated within the beginning of the error range. In other words, the exponential weighting algorithm has a significantly higher positioning accuracy within the error range of 0–1 cm. Therefore, the exponential weighting algorithm demonstrates a clear advantage in the positioning error CDF than the other two algorithms.

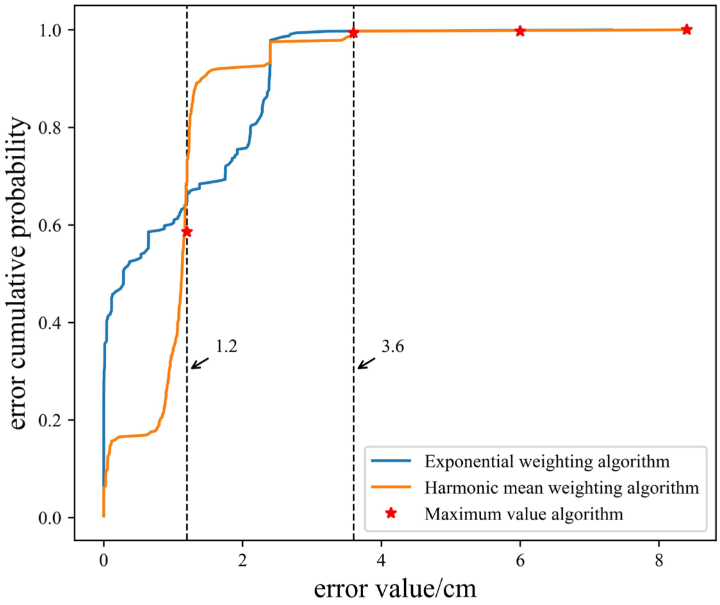

Figure 6. The error cumulative distribution function (CDF) of three different positioning algorithm.

As for the number of detected RFID tags used in the weighting, the AR of the exponential weighting algorithm reaches its maximum when the weighting number is three, and further increases in the weighting number do not have a significant effect on the AR. The AR and GAR of the harmonic mean weighting algorithm reach their maximum when the weighting number is two, but as the weighting number continues to increase, both the AR and GAR tend to decrease. This is because the exponential weighting algorithm exponentially amplifies the weight differences between detected RFID tags with different signal strengths, making the positioning results concentrate near the RFID tag with the strongest signal, which leads to more stable positioning outcomes. The harmonic mean weighting algorithm has less distinction in weights between different signal strength levels. Excessive weighting numbers can introduce more data noise to the positioning, resulting in a decrease in positioning accuracy.

In summary, through experiments on the measurement accuracy of RFID scales and comparative analysis of different positioning algorithms, the best RFID scales hardware composition is the combination of the ceramic antenna KLTX2525 and a dual-tag strip, which is the LALT scheme. The optimal positioning algorithm for RFID scales is the exponential weighting algorithm. The optimal weighting number is three, which means using the top three RFID tags with the highest RSSI signals for weighting. Using this RFID scales hardware composition and the positioning algorithm to measure the depth of concrete vibration, the maximum error in depth measurement is, overall, controllable. There is 99.69% confidence that the vibration depth monitoring error is within 3.6 cm, of which 65.34% of the depth error is within an even smaller range of 1.2 cm.

3.4. On-Site Vibration Depth Monitoring Using RFID Scales

To verify the feasibility of using RFID scales for monitoring the depth of concrete vibration, the monitoring of vibration depth was conducted at a construction site, as shown in Figure 7. Figure 7a shows that when the vibrator is fully inserted into the concrete, the RFID scales mounted on the digital board is monitoring the vibration depth. Figure 7b shows that the digital board hanging at the junction of the vibrator's metal head and the flexible shaft is moving with the vibrator to the next vibration location after the vibrator has been withdrawn from the concrete.

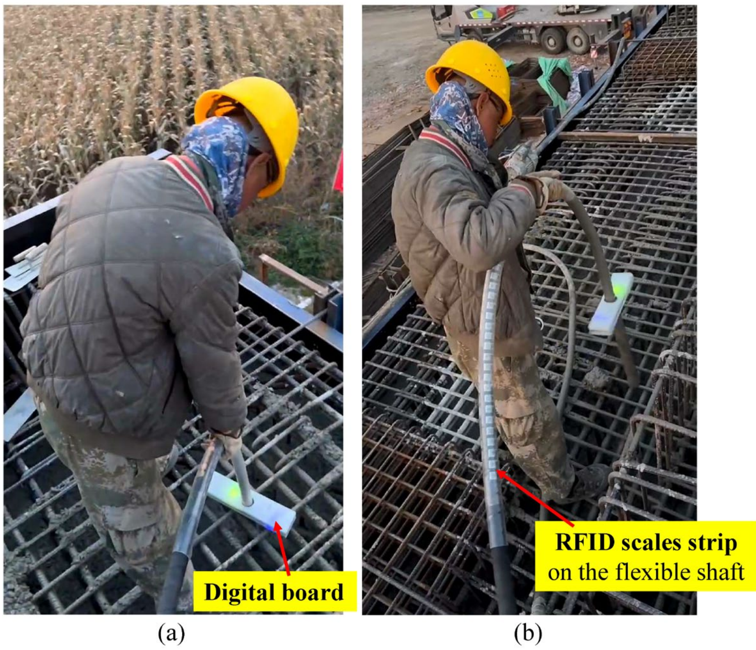

Figure 7. On-site monitoring of vibration depth: (**a**) RFID scales is monitoring the depth; (**b**) RFID scales is moving with the vibrator to the next vibration location.

The concrete vibration depth monitoring device based on RFID scales is shown in Figure 8. The dual-tag strip arranged along the flexible shaft is protected by a transparent layer that is both waterproof and scratch-resistant. The digital board has a waterproof cover with the RFID reader and ceramic antenna KLTX2525 inside. In addition, the data transmission and power supply module on the digital board can transmit the real-time depth data from the RFID scales to a computer terminal.

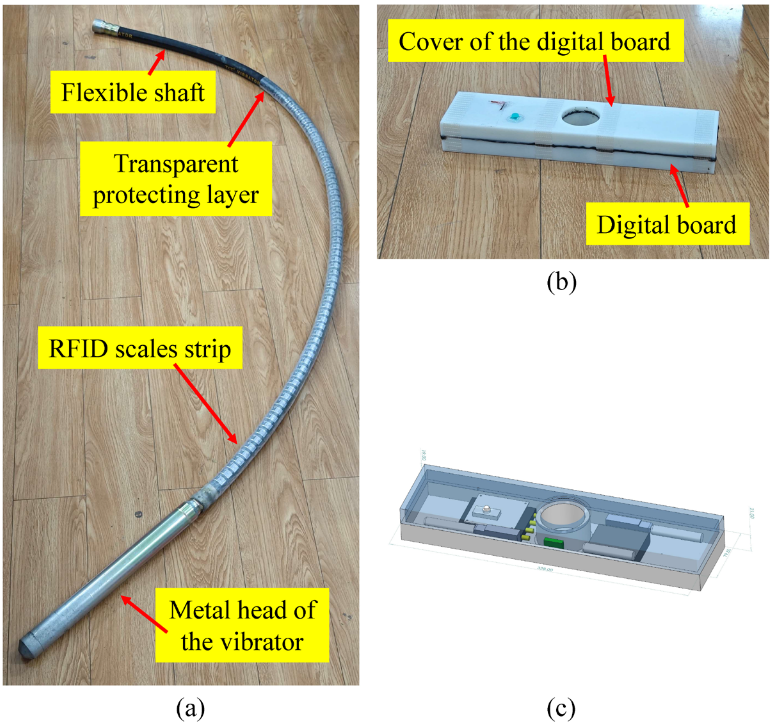

Figure 8. The concrete vibration depth monitoring device based on RFID scales: (**a**) RFID scales strip on the flexible shaft; (**b**) Digital board with the cover; (**c**) 3D model of the digital board.

At the vibration construction site, three different vibration depths of 120 cm, 140 cm, and 160 cm were selected. At each depth, three vibration points were chosen for testing the depth monitoring performance. Figure 9 presents the time-history data of vibration depth monitoring at the three different depths. For each depth, three consecutive vibration depth changes can be clearly observed. The maximum depth value monitored of each vibration and its corresponding time are marked in the figure.

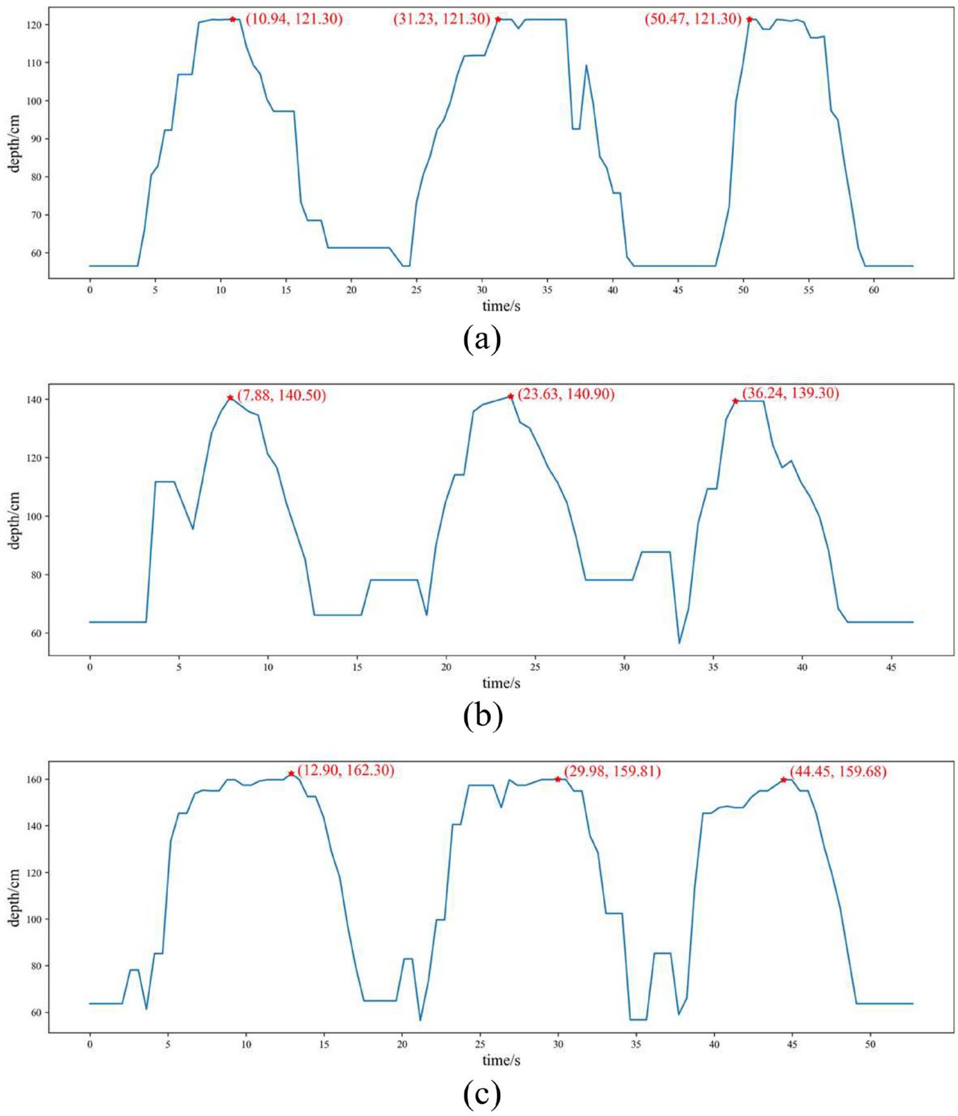

Figure 9. The time-history data of vibration depth monitoring: (**a**) vibration depth of 120 cm; (**b**) vibration depth of 140 cm; (**c**) vibration depth of 160 cm.

By comparing the maximum depth value monitored with the true depth value, the accuracy of the vibration depth monitoring based on the RFID scales in a real vibration construction site can be analyzed. Table 8 shows the depth monitoring errors under different vibration depths. As can be seen from Table 8, most of the depth monitoring errors are within 1.2 cm, with the maximum error being 2.3 cm. All depth monitoring errors are within the acceptable range of 3.6 cm. The results of using the RFID scales to monitor the vibration depth at the construction site are consistent with the AR and GAR of the RFID scales in the experiment in Section 3.2.

Table 8. The depth monitoring errors under different vibration depths.

True Vibration Depth	Depth Monitoring Error/cm		
	The First Vibration	The Second Vibration	The Third Vibration
120 cm	1.3	1.3	1.3
140 cm	0.5	0.9	−0.7
160 cm	2.3	−0.19	−0.32

The application at the vibration construction site has confirmed the feasibility of using RFID scales for monitoring the concrete vibration depth. Indeed, the application scenarios of RFID scales system in engineering sites in this paper are relatively limited. It is worth noting that the performance of RFID scales system may be affected by the dynamic construction site conditions, such as temperature, humidity, vibration, and electromagnetic interference. In the future, it is necessary to conduct on-site applications and tests in various environmental conditions at engineering construction sites to continuously improve and enhance the reliability of the RFID scales positioning systems. Besides achieving the vibration depth control in real time, the depth data from the RFID scales can be used in many ways in the future. By analyzing the starting point of the vibration depth monitoring curve, the time of vibration can be determined. The slope of the vibration depth time-history curve can be used to assess the insertion and withdrawal speeds of the vibrator, which can serve as a quality control index to check the requirement of the quick insertion and slow withdrawal technique in the vibration process.

4. Discussion and Future Outlook

This study is the first attempt to apply an RFID system to address the problem of depth monitoring during concrete vibration. Inspired by the principles of optical and magnetic scales, an RFID scales positioning system is proposed, achieving real-time monitoring of concrete vibration depth with centimeter-level accuracy. Compared to previous research, the following innovations and improvements have been made.

1. The RFID scales positioning system is proposed for the first time. The optimal integration of RFID scales with the hand-held concrete vibrator is explored. The dual-tag strip mounted on the flexible shaft of the vibrator and the ceramic antenna KLTX2525 form the best RFID scales hardware composition, achieving the best depth monitoring accuracy. Because the RFID reader, RFID antenna, and other related electronic modules of the RFID scales are arranged on the digital board, these electronic devices are not directly connected to the vibrator. During vibration construction, the digital board remains outside the concrete, averting any interference from the vibration to the sensors. This ensures the stable operation of the sensors and achieves real-time transmission of monitoring data.
2. The RFID scales can conduct the measurement at a frequency of approximately 3 Hz, satisfying the real-time requirements for monitoring concrete vibration depths. The concrete vibration is a typical cyclical behavior, which usually requires 10–20 s to complete a cycle of vibration. During the process of vibration, the depth of vibration will also exhibit periodic changes. The time of a single detection by the RFID scales is related to the distance from the antenna to the tag and the number of tags identified in a single detection, so the time for each detection is not completely consistent. Experiments have found that the time taken for a single detection is between 0.3 s and 0.4 s, corresponding to a measurement frequency about 3 Hz. For real-time monitoring of concrete vibration depth, the sampling frequency requirement for depth monitoring should, according to the Nyquist–Shannon sampling theorem, be at least twice the frequency of the depth change. The sampling frequency of the RFID scales is around 3 Hz, which is far more than twice the frequency of the vibration depth change.
3. The RFID scales positioning system theoretically has no upper limit for the range of vibration depth monitoring. By arranging an RFID scales strip of the corresponding

length on the flexible shaft, the monitoring of vibration at any depth can be realized. However, it should be noted that the starting location of the RFID scales strip on the flexible shaft, which is where the RFID tag numbered 0 is located, is at the junction of the flexible shaft and the metal head of the vibrator. This means that the starting depth of the depth monitoring by RFID scales is the distance from the tag numbered 0 to the top of the vibrator's metal head. In other words, the RFID scales positioning system is only suited for vibration scenarios where the insertion depth of the vibrator is greater than the length of the vibrator's metal head. Actually, when the depth of concrete needed for vibration is less than the length of the vibrator's metal head, the metal head does not need to be fully immersed into the concrete, and the insertion can be assessed directly through visual observation. During the vibration process, the situations that really require vibration depth monitoring are those where the depth of concrete vibration exceeds the length of the vibrator's metal head; once the metal head is fully immersed in the concrete, the true insertion depth is difficult to judge visually.

4. The feasibility of using the RFID scales for monitoring vibration depth has been verified in a construction site application. In an actual vibration scenario, the flexible shaft of the vibrator inserted into the concrete gets coated with a thin layer of cement mortar. Field measurements have shown that this layer of cement mortar on the vibrator's flexible shaft does not affect the signal reading and accuracy of the RFID scales. Furthermore, since the cement mortar layer covers any marked information on the shaft, controlling the vibration depth by marking labels on the shaft and manual inspection is not feasible. This demonstrates the necessity of digital depth monitoring in vibration construction from another perspective.
5. In this paper, the RFID scales strip is arranged on the outside of the flexible shaft of the vibrator, with a transparent protective layer covered on the scales strip. In the subsequent large-scale engineering application of the proposed RFID scales, when the flexible shaft of the vibrator is manufactured, the RFID scales strips can be embedded within the rubber layer of the flexible shaft, utilizing the rubber layer for better protection. Moreover, the automated damage inspection for the RFID scales strip could be possible based on the identified RFID tags data and the machine learning anomaly detection algorithms. The use of machine learning for automated RFID scales strip damage inspection represents an interesting and worthwhile direction for further research.

In fact, vibration depth monitoring based on the RFID scales is the foundation for a series of subsequent vibration digital monitoring and real-time quality control of concrete vibration. The proposed approach for monitoring concrete vibration depth depends exclusively on the time-history data of the RFID scales. In the future, further research and development can be carried out upon the combination of RFID scales depth monitoring and other monitoring methods.

For example, during the layered vibration process of large-volume concrete, the construction standards require that the metal head of the vibrator must penetrate at least 5 cm into the previous layer of concrete to ensure good interlayer bonding. If the RFID scales-based vibration depth monitoring system proposed in this study can be combined with methods that monitor the working state of the vibrator in real time through parameters such as the electric current and voltage of the vibrator's motor [27], the concrete vibration depth of each layer can be calculated by the working state of the vibrator and the depth of vibration together. Thus, the precise monitoring of the vibration depth for each layer of the large-volume concrete can be achieved. Additionally, by equipping the digital board with sensors such as satellite positioning and UWB positioning module, it is possible to track the location of the digital board. This would enable the monitoring of the horizontal position of the vibration insertion point, thereby realizing the full process digital monitoring of key quality factors in concrete vibration, such as horizontal location, depth, time, and technique. Another possible direction is adapting the RFID scales monitoring system to scenarios where the depth of concrete vibration is less than the length of the vibrator's metal head. Distance sensors can be installed at the bottom of the digital board, such as infrared distance sensor, ultrasonic distance sensor, etc., to measure the distance from the bottom of the digital board to the surface of the concrete. When the insertion depth is less than the length of the vibrator's metal head, the digital board hangs at the junction of the vibrator's metal head and the flexible shaft. Combined with the posture data of the digital board, the depth of the concrete vibrator inserted into the concrete can be calculated in real time.

5. Conclusions

This study fills the research gap in concrete vibration depth monitoring. The digital method for monitoring vibration depth using an RFID system is proposed for the first time. Inspired by the optical and magnetic scales, an RFID scales positioning system is proposed. The RFID scales is integrated with the hand-held vibrator through the digital board, and the RFID scales measurement algorithm is based on the exponential weighting method is illustrated. The principle and hardware composition of the RFID scales are explained in detail. The performance differences between RFID scales composed of different antennas and tags are compared and analyzed. The best RFID scales hardware composition consists of the ceramic antenna KLTX2525 and a dual-tag strip, which can achieve centimeter-level depth monitoring accuracy. The RFID scales measurement algorithm uses the RSSI value of each tag to calculate the weight. The exponential weighting algorithm can eliminate the data noise of the RFID scales during depth monitoring. The optimal weighting number is 3. Under this condition, there is 99.69% confidence that the vibration depth monitoring error is within 3.6 cm, of which 65.34% of the depth error is within an even smaller range of 1.2 cm. The feasibility of using RFID scales for vibration depth monitoring is verified by the application at the vibration construction site. The on-site measured depth error is consistent with the positioning error of the RFID scales in the experiments. This research provides a new perspective and system solution for concrete vibration depth monitoring, broadens the measurable range of depth in vibration monitoring, and improves the quality of concrete vibration for deeper structures.

Author Contributions: Conceptualization, Y.Q. and F.W.; methodology, Y.Q.; software, Y.Q. and X.W.; validation, X.W. and Y.L.; formal analysis, Y.Q. and Y.L.; investigation, H.S.; resources, H.S. and F.W.; data curation, X.W.; writing—original draft preparation, Y.Q.; writing—review and editing, Y.Q. and F.W.; visualization, Y.Q.; supervision, F.W.; project administration, X.W. and F.W.; funding acquisition, X.W., Y.L., H.S. and F.W. All authors have read and agreed to the published version of the manuscript.

Funding: This research was funded by Long Jian Road & Bridge Co., Ltd. Technology Project, grant number 230000100004258220001. The APC was funded by Long Jian Road & Bridge Co., Ltd.

Data Availability Statement: The experiment data used to support the findings of this study are available from the corresponding author upon request.

Conflicts of Interest: Author Xinzhi Wang, Yancheng Liu, and Hongpeng Sun are employed by the company Long Jian Road & Bridge Co., Ltd. The remaining authors declare that the research was conducted in the absence of any commercial or financial relationships that could be construed as a potential conflict of interest. The authors declare that this study received funding from Long Jian Road & Bridge Co., Ltd. The funders had no role in the design of the study; in the collection, analyses, or interpretation of data; in the writing of the manuscript; or in the decision to publish the results.

References

1. Wang, D.; Ren, B.; Cui, B.; Wang, J.; Wang, X.; Guan, T. Real-Time Monitoring for Vibration Quality of Fresh Concrete Using Convolutional Neural Networks and IoT Technology. *Autom. Constr.* **2021**, *123*, 103510. [CrossRef]
2. Petrou, M.F.; Harries, K.A.; Gadala-Maria, F.; Kolli, V.G. A Unique Experimental Method for Monitoring Aggregate Settlement in Concrete. *Cem. Concr. Res.* **2000**, *30*, 809–816. [CrossRef]
3. Gao, X.; Zhang, J.; Su, Y. Influence of Vibration-Induced Segregation on Mechanical Property and Chloride Ion Permeability of Concrete with Variable Rheological Performance. *Constr. Build. Mater.* **2019**, *194*, 32–41. [CrossRef]
4. Nawy, E.G. (Ed.) *Concrete Construction Engineering Handbook*, 2nd ed.; CRC Press: Boca Raton, FL, USA, 2008; ISBN 978-0-8493-7492-0.

5. ACI PRC-309-05: Guide for Consolidation of Concrete. Available online: https://www.concrete.org/store/productdetail.aspx?ItemID=30905&Language=English&Units=US_AND_METRIC (accessed on 8 February 2024).
6. Code for Construction of Concrete Structures. Available online: https://www.chinesestandard.net/China/Chinese.aspx/GB50666-2011 (accessed on 8 February 2024).
7. Li, J.; Tian, Z.; Yu, X.; Xiang, J.; Fan, H. Vibration Quality Evaluation of Reinforced Concrete Using Energy Transfer Model. *Constr. Build. Mater.* **2023**, *379*, 131247. [CrossRef]
8. Li, J.; Tian, Z.; Sun, X.; Ma, Y.; Liu, H.; Lu, H. Modeling Vibration Energy Transfer of Fresh Concrete and Energy Distribution Visualization System. *Constr. Build. Mater.* **2022**, *354*, 129210. [CrossRef]
9. Wang, M.; Yang, X.; Wang, W. Establishing a 3D Aggregates Database from X-Ray CT Scans of Bulk Concrete. *Constr. Build. Mater.* **2022**, *315*, 125740. [CrossRef]
10. Yang, X. Research on the Data Collection and Application Methods of Concealed Construction. Ph.D. Thesis, Harbin Institute of Technology, Harbin, China, 2020. (In Chinese).
11. Tian, Z.; Bian, C. Visual Monitoring Method on Fresh Concrete Vibration. *KSCE J. Civ. Eng.* **2014**, *18*, 398–408. [CrossRef]
12. Gong, J.; Yu, Y.; Krishnamoorthy, R.; Roda, A. Real-Time Tracking of Concrete Vibration Effort for Intelligent Concrete Consolidation. *Autom. Constr.* **2015**, *54*, 12–24. [CrossRef]
13. Quan, Y.; Wang, F. Machine Learning-Based Real-Time Tracking for Concrete Vibration. *Autom. Constr.* **2022**, *140*, 104343. [CrossRef]
14. Tian, Z.; Sun, X.; Su, W.; Li, D.; Yang, B.; Bian, C.; Wu, J. Development of Real-Time Visual Monitoring System for Vibration Effects on Fresh Concrete. *Autom. Constr.* **2019**, *98*, 61–71. [CrossRef]
15. Zhang, W.; Li, Y.; Xie, Q. The influence of vibration depth on formwork lateral pressure of fresh casting concrete. *Ind. Constr.* **2016**, *46*, 110–115. (In Chinese) [CrossRef]
16. Li, W. Experimental study on influential factors of side pressure acting on framework caused by newly concrete pouring. *Railw. Eng.* **2019**, *59*, 37–40+45. (In Chinese)
17. Li, C.; Tanghe, E.; Plets, D.; Suanet, P.; Hoebeke, J.; De Poorter, E.; Joseph, W. ReLoc: Hybrid RSSI-and Phase-Based Relative UHF-RFID Tag Localization with COTS Devices. *IEEE Trans. Instrum. Meas.* **2020**, *69*, 8613–8627. [CrossRef]
18. Buffi, A.; Motroni, A.; Nepa, P.; Tellini, B.; Cioni, R. A SAR-Based Measurement Method for Passive-Tag Positioning with a Flying UHF-RFID Reader. *IEEE Trans. Instrum. Meas.* **2019**, *68*, 845–853. [CrossRef]
19. Cai, H.; Andoh, A.R.; Su, X.; Li, S. A Boundary Condition Based Algorithm for Locating Construction Site Objects Using RFID and GPS. *Adv. Eng. Inform.* **2014**, *28*, 455–468. [CrossRef]
20. Bu, Y.; Xie, L.; Gong, Y.; Wang, C.; Yang, L.; Liu, J.; Lu, S. RF-Dial: An RFID-Based 2D Human-Computer Interaction via Tag Array. In Proceedings of the IEEE INFOCOM 2018—IEEE Conference on Computer Communications, Honolulu, HI, USA, 16–19 April 2018; pp. 837–845.
21. Wang, C.; Liu, J.; Chen, Y.; Liu, H.; Xie, L.; Wang, W.; He, B.; Lu, S. Multi—Touch in the Air: Device-Free Finger Tracking and Gesture Recognition via COTS RFID. In Proceedings of the IEEE INFOCOM 2018—IEEE Conference on Computer Communications, Honolulu, HI, USA, 16–19 April 2018; pp. 1691–1699.
22. Ni, L.M.; Yunhao, L.; Yiu, C.L.; Patil, A.P. LANDMARC: Indoor Location Sensing Using Active RFID. In Proceedings of the 1st IEEE International Conference on Pervasive Computing and Communications, 2003, (PerCom 2003), Fort Worth, TX, USA, 23 March 2003; pp. 407–415.
23. Yang, C.; Wang, X.; Mao, S. SparseTag: High-Precision Backscatter Indoor Localization with Sparse RFID Tag Arrays. In Proceedings of the 16th Annual IEEE International Conference on Sensing, Communication, and Networking (SECON), Boston, MA, USA, 10–13 June 2019; pp. 1–9.
24. Optical Scales. Available online: https://www.willtec.de/en/measure/optical-scales/ (accessed on 8 February 2024).
25. Magnetic DRO Scales. Available online: https://www.touchdro.com/resources/scales/magnetic/overview.html (accessed on 8 February 2024).
26. Álvarez López, Y.; de Cos Gómez, M.E.; Las-Heras Andrés, F. A Received Signal Strength RFID-Based Indoor Location System. *Sens. Actuators A Phys.* **2017**, *255*, 118–133. [CrossRef]
27. Li, J.; Tian, Z.; Sun, X.; Ma, Y.; Liu, H. Working State Determination for Concrete Internal Vibrator Using Genetic Simulated Annealing Clustering Method. *Case Stud. Constr. Mater.* **2022**, *17*, e01163. [CrossRef]